The Influence of the Amine Concentration onto Product Formation: Crystal Structures, Thermal Stability and Spectroscopic Properties of Two New Manganese Thiostannates Obtained under Solvothermal Conditions

Nicole Pienack, Christian Näther, and Wolfgang Bensch

Institute of Inorganic Chemistry, Christian-Albrechts-University of Kiel, Max-Eyth-Straße 2,
24118 Kiel, Germany

Reprint requests to Wolfgang Bensch. Phone: +49 431 880-2419. Fax: +49 431 880-1520.
E-mail: wbensch@ac.uni-kiel.de

Z. Naturforsch. **2008**, *63b,* 1243 – 1251; received August 27, 2008

Two new thiostannates with Mn^{2+} ions were obtained under solvothermal conditions applying different amine concentrations. $[Mn(C_6H_{14}N_2)_2(H_2O)]_2Sn_2S_6$ (**1**) ($C_6H_{14}N_2$ = 1,2-diaminocyclohexane, 1,2-dach) crystallizes in the monoclinic space group $C2/c$ (with a = 23.7500(18), b = 15.5655(16), c = 12.1072(9) Å, β = 113.532(8)°, Z = 8). The second compound, $[Mn(C_6H_{14}N_2)_2]$-$Sn_2S_6 \cdot 2\,C_6H_{15}N_2$ (**2**), crystallizes in the triclinic space group $P\bar{1}$ with a = 7.3019(6), b = 11.1798(9), c = 13.2837(11) Å, α = 76.877(10), β = 74.719(9), γ = 82.972(10)°, Z = 1. Both structures feature $[Sn_2S_6]^{4-}$ anions acting as bidentate ligands and joining the octahedrally coordinated Mn^{2+} cations, but in **1** a molecular complex is formed, whereas in **2** a one-dimensional coordination polymer is observed. In **1** the Mn^{2+} cation has bonds to four N atoms of two 1,2-dach ligands, to one H_2O molecule, and to one S atom of the $[Sn_2S_6]^{4-}$ anion. The $[Sn_2S_6]^{4-}$ anion is located on a center of inversion joining two symmetry related complexes. In **2** Mn^{2+} is surrounded by four N atoms of two 1,2-dach ligands and by two S atoms of two neighboring $[Sn_2S_6]^{4-}$ anions. In contrast to **1** a negatively charged coordination polymer is formed with $[Sn_2S_6]^{4-}$ anions acting as linkers and the Mn^{2+} centered complexes being the nodes. The co-crystallized 1,2-dach molecules are protonated, and they are located between the chains. The first compound was obtained from diluted aqueous solutions of 1,2-dach, and **2** crystallized from solutions containing $< 25\,\%$ H_2O. In both compounds several short S$\cdots$H distances indicate weak hydrogen bonding interactions. Compound **1** is stable up to 121 °C and **2** up to 220 °C. In the Raman spectra of **1** and **2** resonances which are typical for $[Sn_2S_6]^{4-}$ units could be observed. The band gaps are found to be 2.6 eV (477 nm) and 3.1 eV (400 nm) for **1** and **2**, respectively.

Key words: Thiostannates, Solvothermal Syntheses, Crystal Structure, Thermal and Spectroscopic Properties

Introduction

During the last decade new open-framework thiometalate compounds were synthesized following the solvothermal route, and the potential of this approach was recently reviewed [1 – 3]. The structural features as well as the physical and chemical properties of thiometalate networks can be altered by the integration of transition metal (*TM*) ions. Whereas it is not surprising that chalcophilic elements like copper and silver can easily be integrated into thiometalate networks [4 – 8], the incorporation of other transition metal cations is more challenging. Using Co^{2+}, Ni^{2+} or Fe^{2+} and amines as solvents and structure-directing molecules, in most of the cases inorganic anions and $[TM(\text{amine})_x]^{n+}$ complexes as charge compensating cations are found in the reaction products as for example in $[Ni(en)_3]_2Sn_2S_6$ (en = ethylenediamine) and $[Ni(dap)_3]_2Sn_2S_6 \cdot 2\,H_2O$ (dap = diaminopropane) [9]. A few years ago we established a new synthesis strategy using multidentate amines like tren (tren = tris(2-aminoethyl)amine) which form unsaturated transition metal complexes. Such unsaturated $[TM(\text{amine})_x]^{n+}$ complexes can form one or two bonds to the thiometalate network [*e. g.* $[Co(tren)]_2$-Sn_2S_6 [9], $[Ni(tren)]Sb_2S_4$ [10] and $[TM(tren)]Sb_4S_7$

0932–0776 / 08 / 1100–1243 $ 06.00 © 2008 Verlag der Zeitschrift für Naturforschung, Tübingen · http://znaturforsch.com

(*TM* = Mn, Fe, Co, Zn) [11]]. Compared to other transition metals, Mn^{2+} behaves differently and is often integrated into thiometalate networks without usage of a multidentate amine. It seems that Mn^{2+} has a comparable affinity to S and N atoms. A prominent example is the thioantimonate structure family $Mn_2(L)Sb_2S_5$ with L = methylamine (ma), ethylamine (ea), diaminopropane (dap), diethylenetriamine (dien), *N*-methyl-1,3-diaminopropane (mdap) [12–14], ethylenediamine (en) [15] or diaminopentane (dape) [16] where one of the two independent Mn^{2+} ions is coordinated by four S and two N atoms whereas the second is surrounded by six S atoms. Another interesting example is the thioantimonate $[Mn(C_6H_{14}N_2)_3]_2[Mn(C_6H_{14}N_2)_2(SbS_4)_2] \cdot 6\,H_2O$ ($C_6H_{14}N_2$ = 1,2-diaminocyclohexane, 1,2-dach) with one Mn^{2+} ion in an isolated $[Mn(1,2\text{-dach})_3]^{2+}$ cation and another Mn^{2+} ion surrounded by two 1,2-dach ligands and two monodentate $[SbS_4]^{3-}$ units [17]. In the literature only a few Mn thiostannates were reported like $[Mn(en)_3]_2Sn_2S_6$ [18] and $[Mn(dien)_2]_2Sn_2S_6$ [19] with isolated $[Sn_2S_6]^{4-}$ anions, or $([Mn_2(en)_5]Sn_2S_6)_n$ in which Mn^{2+} has bonds to one S atom and 5 N atoms [20]. Recently, we published the first Mn^{2+} containing thiostannate $(1,4\text{-dabH})_2MnSnS_4$ crystallizing in an anionic chain structure with protonated amine molecules as charge compensating cations [21].

During our investigation of the Mn-Sn-S-1,2-diaminocyclohexane system we obtained two thiostannates $[Mn(C_6H_{14}N_2)_2(H_2O)]_2Sn_2S_6$ and $[Mn(C_6H_{14}N_2)_2]Sn_2S_6 \cdot 2\,C_6H_{15}N_2$. Here we report on their syntheses, crystal structures, spectroscopic and thermal properties.

Experimental

Synthesis

General

All chemicals were purchased (see below for purity and source) and used without further purifications. All compounds were prepared under solvothermal conditions in Teflon-lined steel autoclaves (inner volume: 30 mL) using manganese, tin and sulfur. The crystalline products were filtered off after the reactions, washed with water and ethanol and dried in vacuum.

*Synthesis of $[Mn(C_6H_{14}N_2)_2(H_2O)]_2Sn_2S_6$ (**1**)*

1 mmol Sn (99.5 %, Aldrich), 1 mmol Mn (99.5 %, Alfa Aesar) and 4 mmol S in 2.5 mL of 1,2-diaminocyclohexane ($C_6H_{14}N_2$, 1,2-dach) (≥ 99 %, Aldrich) and 2.5 mL of water were reacted for 98 h at 130 °C. In the reaction products dark-brown rods as well as several manganese and tin sulfides were found. The yield of $[Mn(C_6H_{14}N_2)_2(H_2O)]_2Sn_2S_6$ was about 15 % (based on tin).

Table 1. Selected details of the data collection and structure refinement results of the title compounds.

	$[Mn(C_6H_{14}N_2)_2$-$(H_2O)]_2Sn_2S_6$ (**1**)	$[Mn(C_6N_2H_{14})_2]$-$Sn_2S_6 \cdot 2\,C_6N_2H_{15}$ (**2**)
Crystal system	monoclinic	triclinic
Space group	$C2/c$	$P\bar{1}$
a, Å	23.7500(18)	7.3019(6)
b, Å	15.5655(16)	11.1798(9)
c, Å	12.1072(9)	13.2837(11)
α, deg	90	76.877(10)
β, deg	113.532(8)	74.719(9)
γ, deg	90	82.872(10)
V, Å^3	4103.6(6)	1016.36(14)
Z	4	1
$D_{\text{calcd.}}$, g cm^{-3}	1.67	1.54
μ, mm^{-1}	2.1	1.9
Scan range in θ, deg	$2.62 \le 28.16$	$2.72 \le 28.00$
Reflections collected	25198	10307
Independent reflections	4943	4838
Refl. with $F_o \ge 4\sigma(F_o)$	2088	479
Goodness-of-fit on F^2	1.049	0.937
Final $R1/wR2$ $[I \ge 2\sigma(I)]$	0.0381 / 0.0923	0.0370 / 0.0793
Final $R1/wR2$ (all data)	0.0457 / 0.0958	0.0622 / 0.0873
$\Delta\rho_{\text{fin}}$ (max / min), e Å^{-3}	1.39 / −1.20	0.83 / −1.21

*Synthesis of $[Mn(C_6H_{14}N_2)_2]Sn_2S_6 \cdot 2\,C_6H_{15}N_2$ (**2**)*

1 mmol Sn, 1 mmol Mn and 4 mmol S in 5 mL of 1,2-dach were reacted for 98 h at 130 °C. In the reaction products yellow needles were found in a yield of approximately 15 % (based on Sn) whereas metal sulfides formed the main part of the products.

The crystals were manually separated, and the homogeneity of the compounds was confirmed by X-ray powder diffraction and CHN analyses: **1**: calcd. C 27.9, H 5.8, N 10.9; found C 26.4, H 5.7, N 10.4; **2**: calcd. C 30.6, H 6.2, N 11.9; found C 30.1, H 6.2, N 11.6.

Structure determination

The intensity data were collected using a Stoe IPDS-1 (Imaging Plate Diffraction System) with MoK_α radiation at r. t. for **1** and **2**. The structures were solved with Direct Methods using the program SHELXS-97 [22], and the refinements were done against F^2 with SHELXL-97 [23]. For all non-hydrogen atoms anisotropic displacement parameters were used. The hydrogen atoms of the amines and of the water molecules in **1** were positioned with idealized geometry and refined using a riding model and fixed isotropic displacement parameters. To account for the disorder of the amine in compound **2**, the structure refinement was done using a split model. Selected refinement results are summarized in Table 1.

CCDC 701654 (**1**) and CCDC 701655 (**2**) contain the supplementary crystallographic data for this paper. These data can be obtained free of charge from The Cambridge Crystallographic Data Centre *via* www.ccdc.cam.ac.uk/data_request/cif.

Thermal investigations

The thermal measurements were performed on a Netzsch STA 429 DTA-TG device. The samples were heated to 600 °C at a rate of 4 $\mathrm{K\,min^{-1}}$ under a flow of argon (75 $\mathrm{mL\,min^{-1}}$) in Al_2O_3 crucibles. The TG data were corrected for buoyancy and current effects.

Infrared spectroscopy

MIR spectra (450 – 3000 $\mathrm{cm^{-1}}$) were recorded with an ATI Mattson Genesis spectrometer. In the IR spectra the absorptions located at 3271 (m, -NH stretch, $-NH_2$), 3199 (w, -NH stretch, $-NH_2$), 3118 (m, -NH stretch, $-NH_2$), 2927 (s, $-CH_2$; m-s, -NH stretch), 2852 (m, -NH stretch), 1625 (m, -CC), 1574 (s, $-NH_2$), 1444 (s, -CH, $-CH_2$), 1349 (m, -CN), 1227 (w, -CN), 1139 (w, -CN), 1108 (m, -CN) and 1008 (s, -CN) $\mathrm{cm^{-1}}$ for **1** can be assigned to the diaminocyclohexane. The corresponding absorptions for **2** are: 3443 (m, -NH stretch (asym), $-NH_2$), 3299 (s, -NH stretch, $-NH_2$), 3243 (s, -NH stretch, $-NH_2$), 3137 (m, -NH stretch, $-NH_3^+$), 2924 (s, $-CH_2$; m-s, -NH stretch), 2852 (s, $-CH_2$; m-s, -NH stretch), 2720 (m, -NH stretch, $-NH_3^+$), 2645 (m, -NH stretch, $-NH_3^+$), 2503 (s, -NH stretch (asym), $-NH_3^+$), 2022 (m, $-NH_3^+$ overtone), 1580 (s, $-NH_2$), 1508 (s, $-NH_3^+$ deformation (sym)), 1451 (s, -CH, $-CH_2$), 1379 (s, -CN), 1119 (s, -CN) and 1004 (s, -CN) $\mathrm{cm^{-1}}$.

Raman spectroscopy

Raman spectra were recorded with a Bruker IFS 66 Fourier transform Raman spectrometer (wavelength: 541.5 nm) in the region from 100 to 3500 $\mathrm{cm^{-1}}$.

UV/Vis spectroscopy

UV/Vis spectroscopic investigations were carried out at r. t. using a UV/Vis/NIR two-channel spectrometer Cary 5 from Varian Techtron Pty., Darmstadt. The optical properties of the compounds were investigated by analyzing the UV/Vis reflectance spectra of the powdered samples (with $BaSO_4$ powder used as reference material). The absorption data were calculated applying the Kubelka-Munk relation for diffuse reflectance data. For **1** E_g amounts to 2.6 eV (477 nm), and the value for **2** is 3.1 eV (400 nm).

EDX experiments

Scanning electron microscopy investigations and energy dispersive analysis of X-rays (EDX) were carried out with a Philips Environmental Scanning Electron Microscope ESEM XL30 equipped with an EDAX detector.

Results and Discussion

Syntheses

Despite a large number of attempted syntheses, varying several experimental parameters like temperature or time, the low yields for the two new compounds could not be improved. This observation is not unusual, and several other reaction parameters may have to be also varied. But such further variations are time consuming, and one cannot be sure that the yield will be significantly enhanced. Nevertheless, the title compounds are interesting examples demonstrating the influence of the concentration of the amine onto the stoichiometry of the product. In concentrated 1,2-dach solution the compound $[Mn(C_6H_{14}N_2)_2]Sn_2S_6 \cdot 2\,C_6H_{15}N_2$ (**2**) is formed with the Mn^{2+} cation being octahedrally surrounded by four N and two S atoms. Dilution of 1,2-dach with water results in the crystallization of $[Mn(C_6H_{14}N_2)_2(H_2O)]_2Sn_2S_6$ (**1**) where the octahedral environment of the Mn^{2+} ion contains four N atoms, one O and one S atom. In the concentration range from 12.5 up to 62.5 % aqueous 1,2-dach solution only **1** is obtained, and a mixture of both compounds is formed applying a 75 % 1,2-dach solution. Above this concentration the water containing thiostannate is not observed, and **2** crystallizes.

Crystal structures

$[Mn(C_6H_{14}N_2)_2(H_2O)]_2Sn_2S_6$ (**1**) crystallizes in the monoclinic space group $C2/c$ with four formula units in the unit cell while $[Mn(C_6H_{14}N_2)_2]Sn_2S_6 \cdot 2\,C_6H_{15}N_2$ (**2**) crystallizes in the triclinic space group $P\bar{1}$ with one formula unit in the unit cell. Both structures consist of $[Sn_2S_6]^{4-}$ anions and charge-compensating Mn^{2+}-centered complexes. All atoms are located on general positions except Mn in **2** which is located on a crystallographic center of inversion. The $[Sn_2S_6]^{4-}$ bi-tetrahedron (Fig. 1) is formed by two symmetry related edge-sharing SnS_4 tetrahedra, and this anion is very common for thiostannates [9, 18 – 20].

The values for the terminal Sn–S_t bond lengths of 2.3294(10) and 2.3373(10) Å are shorter than the

Table 2. Selected bond lengths (Å) and angles (deg) of compounds **1** and **2**.

	1	**2**
Sn–S1	2.3561(9)	2.3432(10)
Sn–S2	2.3294(10)	2.3373(10)
Sn–S3	2.4582(10)	2.4462(11)
Sn–S3[a]	2.4415(9)	2.4454(12)
S1–Sn–S2	112.25(3)	117.27(4)
S1–Sn–S3	109.37(4)	108.22(4)
S2–Sn–S3	114.76(4)	111.68(4)
S1–Sn–S3[a]	113.02(4)	112.59(4)
S2–Sn–S3[a]	113.07(3)	110.78(4)
S3–Sn–S3[a]	92.99(3)	93.82(4)
Sn–S3–Sn[a]	87.01(3)	86.18(4)
Mn1–N1	2.279(3)	2.267(3)
Mn1–N2	2.297(4)	2.266(4)
Mn1–N3	2.268(3)	
Mn1–N4	2.281(3)	
Mn1–S1	2.5707(10)	2.6888(11)
Mn1–O1	2.302(3)	

[a] Symmetry operations: **1**: $0.5 - x$, $0.5 - y$, $1 - z$; **2**: $-x$, $1 - y$, $1 - z$.

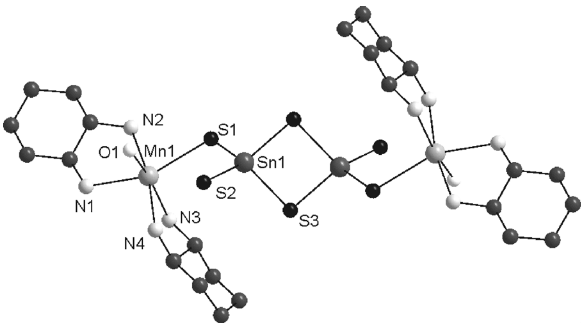

Fig. 1. The structure of $[Mn(C_6H_{14}N_2)_2(H_2O)]_2Sn_2S_6$ (**1**) with atom labeling. Note that H atoms are omitted and C atoms are not labeled.

bridging Sn–S_b bonds with values from 2.4415(9) to 2.4582(10) Å (Table 2).

The S(1) atoms have a bond to the Mn^{2+} cation but the Sn–S bond lengths of 2.3561(9) (**1**) and 2.3432(10) Å (**2**) are not affected, and the values are in the same range like those reported for discrete $[Sn_2S_6]^{4-}$ anions. The S_b–Sn–S_b angles of the Sn_2S_2 rings are 92.99(3) (**1**) and 93.82(4)° (**2**) and are larger than the Sn–S_b–Sn angles [87.01 (**1**) and 86.18° (**2**)]. The other angles around the Sn^{4+} ions range from 108.24(5) to 117.27(4)° (Table 2) indicating a severe deviation from the ideal geometry, but all values match well with those reported in the literature [9, 24].

In both compounds the Mn^{2+} cations are in a distorted octahedral coordination. In **1** the Mn^{2+} ion is surrounded by four N atoms of two amine molecules, one S atom of the $[Sn_2S_6]^{4-}$ anion and one O atom of a water molecule giving the formula $[Mn(C_6H_{14}N_2)_2(H_2O)]^{2+}$ (Fig. 1). In contrast, in **2** the Mn^{2+} cation is in the environment of four N atoms of two ligands and two S atoms of neighboring $[Sn_2S_6]^{4-}$ anions yielding $[Mn(C_6H_{14}N_2)_2S_2]$ as the formula. In **1** the $[Sn_2S_6]^{4-}$ anion is located on a center of inversion and acts as a bidentate ligand connecting two symmetry-related $[Mn(C_6H_{14}N_2)_2(H_2O)]^{2+}$ complexes forming neutral $[Mn(C_6H_{14}N_2)_2(H_2O)]_2Sn_2S_6$ moieties. In **2** the position of the H_2O molecule is empty allowing bond formation to another $[Sn_2S_6]^{4-}$ anion yielding a coordination polymer with the Mn^{2+} complexes as nodes and the anions as linkers (Fig. 2).

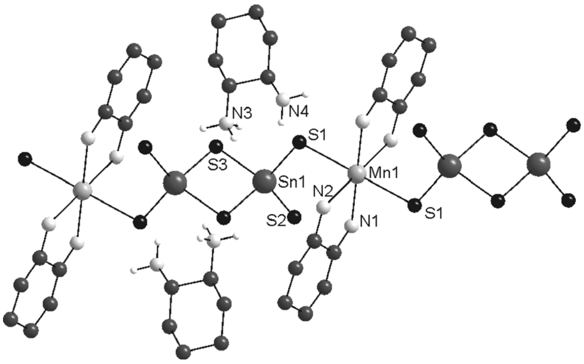

Fig. 2. Part of the crystal structure of compound **2** showing the $\{[Mn(C_6H_{14}N_2)_2]Sn_2S_6\}$ chain and the isolated 1,2-dach molecules. Note that only the H atoms of the isolated 1,2-dach molecules are shown.

In compound **1** the Mn–N bond lengths (2.268(3) – 2.297(4) Å, Table 2), the Mn–N–Mn angles ranging from 74.85(13) to 168.43(14)°, the Mn–S bond of 2.5707(10) Å as well as the Mn–O bond of 2.302(3) Å are in the range as reported for other compounds like $C_9H_{23}N_3OMnS_4$ [25], $[Mn(C_6H_{18}N_4)(C_6H_{19}N_4)]SbS_4$ ($C_6H_{18}N_4$ = tren) and $[Mn(C_6H_{14}N_2)_3]_2[Mn(C_6H_{14}N_2)_2(SbS_4)_2] \cdot 6\,H_2O$ [17].

In **2** the Mn–N bonds are identical (2.266(4) and 2.267(3) Å, bite angle N–Mn–N: 77.76(13)°) and shorter than in **1**. In contrast, the Mn–S bond length of 2.6888(11) Å (Table 2) is about 0.12 Å longer than in **1**. Sterical requirements of the amine may explain the weakening of the Mn–S interaction. The enlargement of the Mn–S bond length is accompanied by a shortening of the Mn–N bonds. A similar phenomenon was observed in the thioantimonate family $Mn_2(L)Sb_2S_5$ [12, 13, 16] where Mn–S distances up to 3.185 Å for L = mdap were observed [14, 16].

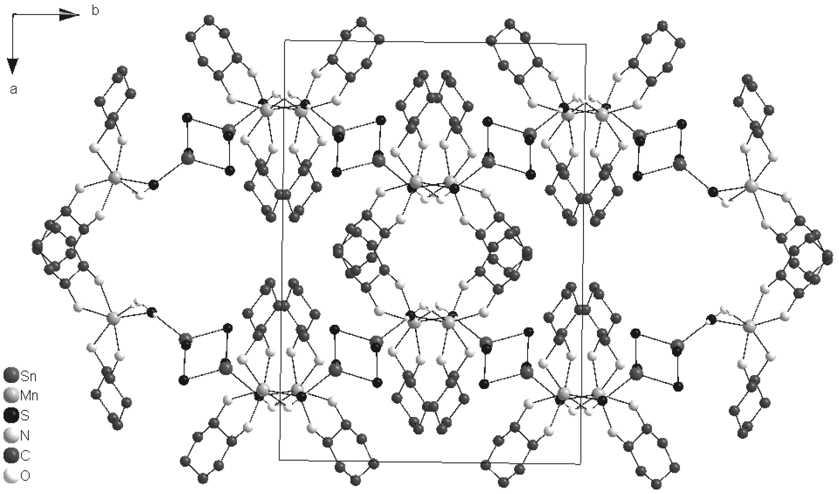

Fig. 3. Arrangement of the [Mn-$(C_6H_{14}N_2)_2(H_2O)]_2Sn_2S_6$ units in compound **1** (view along the *c* axis). H atoms are omitted for clarity.

Table 3. Interatomic S···H distances (Å) and angles (deg) indicating hydrogen bonding interactions.

Distances	1	2	Angles	1	2
S1··· H–N1	2.750	–	S1–H–N1	158.75	–
S1··· H–O1	2.267	–	S1–H–O1	166.30	–
S1··· H–N3	–	2.522	S1–H–N3	–	147.48
S2··· H–N1	2.743	2.686[a]	S2–H–N1	167.23	170.41
S2··· H–N2	–	2.799	S2–H–N2	–	155.29
S2··· H–N3	2.681	2.449	S2–H–N3	163.82	168.33
S2··· H–N3	2.664	2.427	S2–H–N3	156.86	163.79
S2··· H–N4	2.628[a]	2.917	S2–H–N4	157.04	136.05
S2··· H–O1	2.243[a]	–	S2–H–O1	169.41	–
S3··· H–N4	2.953	–	S3–H–N4	149.49	–

[a] Intramolecular contacts.

The N–Mn–S angles are in the range from 84.60(9) to 95.40(9)° evidencing a severe distortion of the octahedral environment.

In **1** the $[Mn(C_6H_{14}N_2)_2(H_2O)]_2Sn_2S_6$ moieties are stacked onto each other to form rods along [$\bar{1}$10] and along [001]. Within the (001) plane a layer-like arrangement of the complexes occurs with neighboring molecules being rotated by 90° (Fig. 3). The dimensions of the channels formed by four complexes (see center of the unit cell) are about $6.2 \cdot 5.2$ Å^2.

In **1** the H_2O molecules and N(1), N(3), and N(4) are involved in intra- and intermolecular hydrogen bonding interactions (see Table 3). One of the H atoms of H_2O has a short distance to the terminal S(2) atom and the other an interaction with S(1) of a neighboring molecule. The S(2) atom is involved in five S···H interactions of which two are intramolecular and three connect to two adjacent $[Mn(C_6H_{14}N_2)_2(H_2O)]_2Sn_2S_6$ units. The bridging S(3) atom has only one such interaction to a neighboring moiety, and S(1) has also one contact to this neighbor.

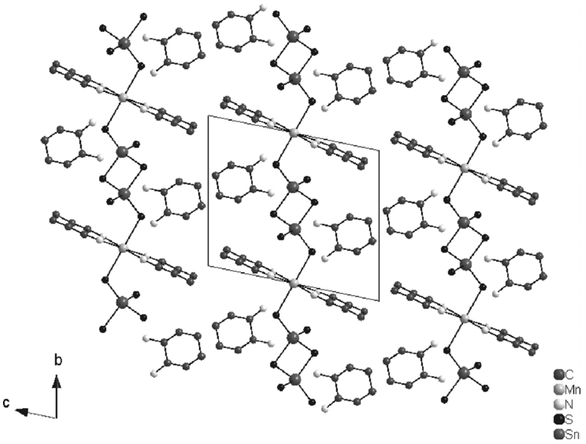

Fig. 4. Arrangement of the chains and the amine molecules in compound **2** (view along [100]). Hydrogen atoms are omitted for clarity.

In **2** the anionic chains are running along [010]. The void space generated by neighboring chains is occupied by the 1,2-dach molecules. Charge neutrality requires protonated amine molecules in the second compound where these are located next to the $[Sn_2S_6]^{4-}$ anions (Fig. 4).

It is obvious that the different arrangements are due to the spatial requirements of the cations and anions. Like for **1** several S atoms of **2** are involved in S···H interactions (Table 3), but the bridging S(3) atom is not part of such contacts. All three H atoms of the $N(3)H_3$ group show S···H bonding interactions with S atoms of two adjacent chains,

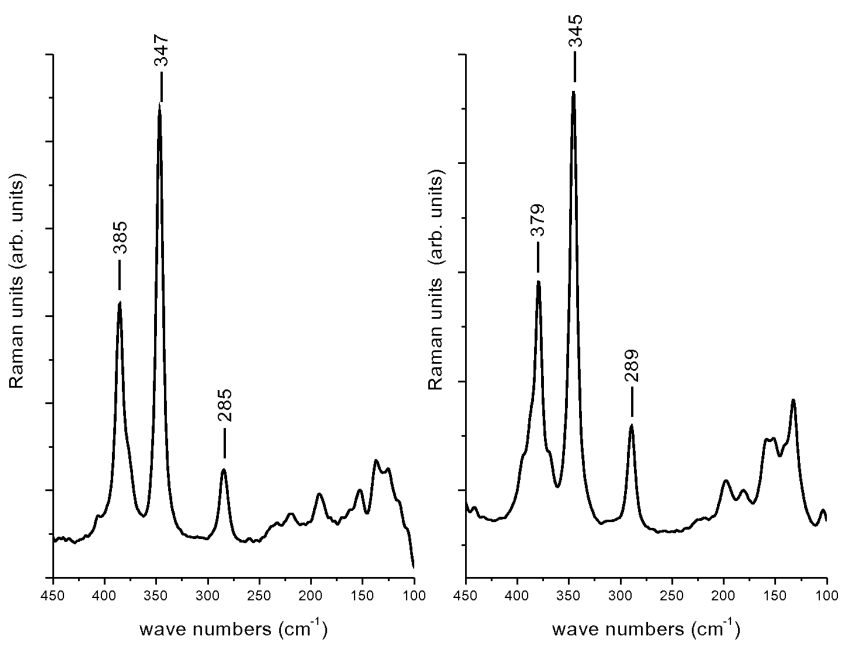

Fig. 5. The Raman spectra of compounds **1** and **2**. The wave numbers of the most prominent lines are given in the spectra.

whereas only one H atom of N(4)H_2 has such a contact (Table 3).

Spectroscopic properties

Raman spectroscopy

The interesting region of the Raman spectra ranges from 400 to 100 cm^{-1} where the Sn–S resonances are located (Fig. 5). Spectral data for the $[Sn_2S_6]^{4-}$ anion are well documented and were reported in many publications, as for example in [9] or for $Na_4Sn_2S_6 \cdot 14\,H_2O$ in ref. [26]. The assignment of the modes was made based on these published data (Table 4).

The resonances of the symmetric Sn–S_t stretching modes are found around 380 cm^{-1}. In compounds **1** and **2** the Sn–S_t bond lengths range from 2.3294(10) to 2.3375(11) Å, and therefore the lines observed in the spectra are slightly shifted [385 cm^{-1} (**1**) and 379 cm^{-1} (**2**)]. The Sn–S_b vibrations are located at lower wave numbers at about 347 cm^{-1} (**1**) and 345 cm^{-1} (**2**). The resonances at 285 cm^{-1} (**1**) and 289 cm^{-1} (**2**) are caused by a Sn_2S_2 ring vibration. The energy differences between the resonances in **1** and **2** as well as to the data reported for $Na_4Sn_2S_6 \cdot 14\,H_2O$ are caused by slightly differing bond lengths and angles. Below 200 cm^{-1} deformation vibrations occur as well as resonances for lattice vibrations. A detailed assignment is not unambiguous, but in the literature the lines at about 190 and 130 cm^{-1} were interpreted as SnS_2 wagging and twisting modes.

Table 4. Data of the Raman lines of $Na_4Sn_2S_6 \cdot 14\,H_2O$, $[Mn(C_6H_{14}N_2)_2(H_2O)]_2Sn_2S_6$ (**1**) and $[Mn(C_6N_2H_{14})_2]$-$Sn_2S_6 \cdot 2\,C_6N_2H_{15}$ (**2**) in cm^{-1}.

$Na_4Sn_2S_6 \cdot 14\,H_2O$[a]	**1**	**2**
377	385	379
341	347	345
281	285	289
190	–	198
151	153	152
136	137	132

[a] Data from ref. [26].

Thermal investigations

Compound **1** decomposes in three steps with a total weight loss of 48.6 % which is accompanied by three endothermic signals with peak temperatures at T_p = 121, 286 and 321 °C (Fig. 6).

The first step corresponds to the removal of water. Unfortunately, the following two thermal reactions are very close preventing a more detailed study of the decomposition mechanism. In the X-ray powder pattern of the decomposition product obtained at 600 °C MnS and SnS could be identified, and the elemental analysis shows a few percent of CHN in the residue. The calculated weight loss of 53.5 % for the decomposition

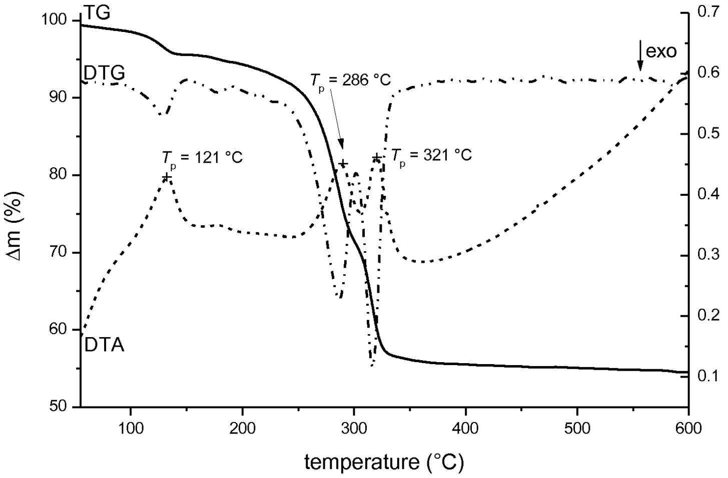

Fig. 6. DTA-TG-DTG curves of compound **1**. The peak temperatures T_p are indicated for the three thermal events.

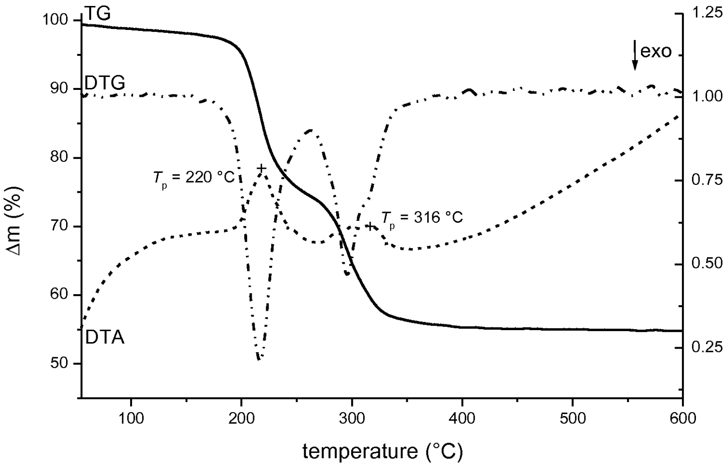

Fig. 7. DTA-TG-DTG curves of compound **2**. The peak temperatures for the two endothermic events are indicated.

according to the formal equation

$$[\mathrm{Mn(C_6H_{14}N_2)_2(H_2O)}]_2\mathrm{Sn_2S_6} \rightarrow 2\mathrm{MnS} + 2\mathrm{SnS} + 2\mathrm{H_2O} + 2\mathrm{H_2S} + 4\mathrm{C_6H_{12}N_2}$$

is larger than the observed value of 48.6 % which could be explained with the CHN contamination of the decomposition product.

Compound **2** decomposes in two steps with a total weight loss of 47.9 % with corresponding endothermic events at T_p = 220 and 316 °C (Fig. 7).

The first step with an onset temperature of T_{onset} = 198 °C and a weight loss of approximately 25 % matches with the loss of two molecules 1,2-dach. The second step is accompanied by a mass loss of about 22.9 % and a broad endothermic signal indicating that there are some very close steps which cannot be resolved. Again, only reflections of MnS and SnS are present in the X-ray powder pattern after the decomposition, and a few percent of CHN can be found in the final black residue. One can expect that the weight loss is due to the emission of 1,2-dach molecules and H_2S. The moderate deviation of the experimentally determined mass loss from the expected value (55.4 %) can be explained with the contamination of the residue. An interruption of the thermal reaction at 220 °C yields a light brownish powder. In the X-ray powder pattern reflections of MnS and SnS were found as well as some reflections which cannot be identified. The elemental analysis gives an overall formula "$[\mathrm{Mn(C_6H_{14}N_2)_2}]\mathrm{SnS_3}$". It can be assumed that in the first step the previously protonated amine molecules are removed. Indeed, in the IR spectrum (Fig. 8) of the intermediate of the thermal decomposition reaction the absorptions corresponding to

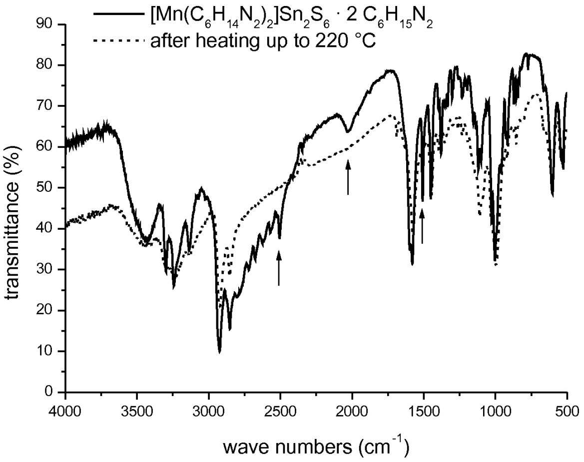

Fig. 8. Comparison of MIR spectra of compound **2** as synthesized and after heating up to 220 °C. Absorptions of the protonated amino groups (-NH_3^+) in the starting material are marked.

the protonated amino groups (-NH_3^+) are missing, but the following modes observed at 3292 (w), 3207 (w), 3134 (w), 2923 (s), 2855 (s), 1688 (m), 1575 (s), 1445 (s), 1396 (m), 1354 (w) and 1110 (s) cm^{-1} can be assigned to the diaminocyclohexane (see Experimental Section infrared spectroscopy).

Conclusions

The successful isolation of the title compounds highlights the synthetic power of the solvothermal approach. From a diluted 1,2-dach solution, $[Mn(C_6H_{14}N_2)_2(H_2O)]_2Sn_2S_6$ (**1**) was obtained with the Mn^{2+} cation coordinated to three different ligands. The coordination of H_2O to Mn^{2+} is a highly interesting observation and to the best of our knowledge was not previously observed in transition metal thiostannate chemistry. Normally water co-crystallizes as crystal water, and the transition metal cations have only bonds to the N atoms of the amine and/or to S atoms of the thiostannate units. The Mn^{2+} cation seems to be unique in the series of transition metal cations with respect to bonding affinities to N and S, as mentioned in the introduction. The isolation of compound **1** further suggests that under special synthetic conditions Mn^{2+} also coordinates to O atoms. Whereas in **1** discrete molecules are observed, the structure of compound **2** can be viewed as a one-dimensional coordination polymer with the Mn^{2+}-centered cations as the nodes and the $[Sn_2S_6]^{4-}$ anions acting as linkers. Comparing the two structures it appears that the removal of the H_2O ligand opens a second binding site for an S atom of an $[Sn_2S_6]^{4-}$ anion. The $\{[Mn(C_6H_{14}N_2)_2]Sn_2S_6\}^{2-}$ chain requires charge compensation which is achieved by the presence of protonated amine molecules. The isolation of two new thiostannates by simply changing the concentration of the structure-directing molecules in the solvent highlights the large synthetic potential of the solvothermal route. Often such dilution experiments are performed to increase the yield of a compound. But new compounds can also be formed and prominent examples are the series of $[Ni(dien)]^{2+}$ complexes (dien = diethylenetriamine) containing thioantimonates(III) [27 – 30]. These thioantimonates were obtained at the same temperature by varying the concentration of the amine. The reason for this finding is that the dilution of an amine not only changes the pH value but also several other important factors like viscosity, redox potential, boiling point *etc*. More syntheses with a systematic variation of the amine concentration may also yield new thiostannates. Such experiments with different amines are currently under way in our laboratory.

Acknowledgement

Financial support by the State of Schleswig-Holstein and the Fonds der Chemischen Industrie is gratefully acknowledged.

---

[1] W. S. Sheldrick, M. Wachhold, *Angew. Chem.* **1997**, *109*, 214 – 234; *Angew. Chem. Int. Ed. Engl.* **1997**, *36*, 206 – 224.
[2] A. K. Cheetham, G. Férey, T. Loiseau, *Angew. Chem.* **1999**, *111*, 3466 – 3492; *Angew. Chem. Int. Ed. Engl.* **1999**, *38*, 3268 – 3292.
[3] T. Jiang, G. A. Ozin, *J. Mater. Chem.* **1998**, *8*, 1099 – 1108.
[4] N. Pienack, W. Bensch, *Z. Anorg. Allg. Chem.* **2006**, *632*, 1733 – 1736.
[5] N. Pienack, C. Näther, W. Bensch, *Solid State Sci.* **2007**, *9*, 100 – 107.
[6] V. Spetzler, H. Rijnberk, C. Näther, W. Bensch, *Z. Anorg. Allg. Chem.* **2004**, *630*, 142 – 148.
[7] V. Spetzler, C. Näther, W. Bensch, *Inorg. Chem.* **2005**, *44*, 5805 – 5812.
[8] V. Spetzler, C. Näther, W. Bensch, *J. Solid State Chem.* **2006**, *179*, 3541 – 3549.
[9] M. Behrens, S. Scherb, C. Näther, W. Bensch, *Z. Anorg. Allg. Chem.* **2003**, *629*, 1367 – 1373.

[10] R. Stähler, W. Bensch, *Eur. J. Inorg. Chem.* **2001**, 3073 – 3078.

[11] M. Schaefer, R. Stähler, W. R. Kiebach, C. Näther, W. Bensch, *Z. Anorg. Allg. Chem.* **2004**, *630*, 1816 – 1822.

[12] W. Bensch, M. Schur, *Eur. J. Solid State Inorg. Chem.* **1996**, *33*, 1149 – 1160.

[13] M. Schur, C. Näther, W. Bensch, *Z. Naturforsch.* **2001**, *56b*, 79 – 84.

[14] L. Engelke, R. Stähler, M. Schur, C. Näther, W. Bensch, R. Pöttgen, M. H. Möller, *Z. Naturforsch.* **2004**, *59b*, 869 – 876.

[15] M. Schur, W. Bensch, *Z. Naturforsch.* **2002**, *57b*, 1 – 7.

[16] A. Puls, C. Näther, W. Bensch, *Z. Anorg. Allg. Chem.* **2006**, *632*, 1239 – 1243.

[17] M. Schaefer, L. Engelke, W. Bensch, *Z. Anorg. Allg. Chem.* **2003**, *629*, 1912 – 1918.

[18] D. X. Jia, Y. Zhang, J. Dai, Q. Y. Zhu, X. M. Gu, *Z. Anorg. Allg. Chem.* **2004**, *630*, 313 – 318.

[19] M. L. Fu, G. C. Guo, B. Liu, A. Q. Wu, J. S. Huang, *Chin. J. Inorg. Chem.* **2005**, *21*, 25 – 29.

[20] X. M. Gu, J. Dai, D. X. Jia, Y. Zhang, Q. Y. Zhu, *Cryst. Growth Des.* **2005**, *5*, 1845 – 1848.

[21] N. Pienack, K. Möller, C. Näther, W. Bensch, *Solid State Sci.* **2007**, *9*, 1110 – 1114.

[22] G. M. Sheldrick, SHELXS-97, Program for the Solution of Crystal Structures, University of Göttingen, Göttingen (Germany) **1997**.

[23] G. M. Sheldrick, SHELXL-97, Program for the Refinement of Crystal Structures, University of Göttingen, Göttingen (Germany) **1997**.

[24] J. Li, B. Marler, H. Kessler, M. Soulard, S. Kallus, *Inorg. Chem.* **1997**, *36*, 4697 – 4701.

[25] K. Wieghardt, U. Bossek, B. Nuber, J. Weiss, *Inorg. Chim. Acta* **1987**, *126*, 39 – 42.

[26] B. Krebs, S. Pohl, W. Schiwy, *Angew. Chem.* **1970**, *21*, 884 – 885; *Angew. Chem., Int. Ed. Engl.* **1970**, *9*, 897 – 898.

[27] W. Bensch, C. Näther, R. Stähler, *Chem. Commun.* **2001**, 477 – 478.

[28] R. Stähler, W. Bensch, *Z. Anorg. Allg. Chem.* **2002**, *628*, 1657 – 1662.

[29] R. Stähler, B.-D. Mosel, H. Eckert, W. Bensch, *Angew. Chem.* **2002**, *114*, 4671 – 4673; *Angew. Chem. Int. Ed.* **2002**, *41*, 4487 – 4489.

[30] R. Stähler, C. Näther, W. Bensch, *J. Solid State Chem.* **2003**, *174*, 264 – 275.